Formation and significance of topologically close-packed Laves phases in refractory high-entropy alloys

Farzaneh Zareipour[a], Hamed Shahmir[a,*] Yi Huang[b]

[a] *Department of Materials Engineering, Tarbiat Modares University, Tehran, Iran*
[b] *Department of Design and Engineering, Bournemouth University, Bournemouth, UK*

Abstract

Refractory high-entropy alloys (RHEAs) inherently have a high potential to form topologically close-packed (TCP) Laves phases. Phase engineering to control the amount and type of TCP-Laves phases plays an important role in physical and mechanical properties of RHEAs. The present investigation addressed key parameters to TCP-Laves phase formation in RHEAs by considering thermodynamic calculations and empirical relations. Two novel TiVCrZrCo and TiVCrZrFe RHEAs were designed and fabricated as alloy models with high melting points (>2000 K) and relatively low density (~6.5 $g.cm^{-3}$) with multiphase microstructure including BCC matrix together with C14 and C15 Laves phases. Existence of atoms such as V, Co, Cr and Fe together with Zr, Ti, Nb and Hf refractory elements promote TCP-Laves phase formation. Very negative values for mixing enthalpy of atom pairs (ΔH_{mix}) and remarkable differences between atomic sizes of the constitutive elements (δ) are key factors in Lave phase formation in multicomponent alloys. The empirical parameters including ΔH_{mix} and δ must be in the defined range of $-20 \leq \Delta H_{mix} \leq -3$ $kJ.mol^{-1}$ and $4 < \delta < 10$ to appear Laves phase in the microstructures of HEAs. TCP-Laves phase formation led to increase and decrease in hardness and fracture toughness, significantly. The understanding of key factors in RHEAs design can lead to phase engineering and the fabricated alloys with a desirable amount of TCP-Laves phase, which are suited for hydrogen storage applications or for applications in harsh operating environments exposed to high temperatures, irradiations, wear, and erosion.

Keywords: Refractory high-entropy alloy; Alloy design; Topologically close-packed phase; Laves phase; Microstructure engineering; Hydrogen storage.

[*]Corresponding author. Tel.: 982182883305 E-mail address: shahmir@modares.ac.ir

1. Introduction

Refractory high-entropy alloys (RHEAs) containing refractory elements such as W, Nb, Mo, Zr, Ta, Hf, V, Cr and Ti in near-equiatomic or equiatomic compositions were introduced to the engineering world as potential materials to substitute the conventional materials for harsh operating environment [1,2]. These alloys are the subclass of high-entropy alloys (HEAs) which have been studied significantly during the last two decades due to their main important advantage which is formation of a solid solution with simple crystal structure in a wide temperature range [3–5]. These RHEAs possess remarkable high temperature mechanical properties such as high strength, high hardness and high wear resistance [6,7]. Moreover, good oxidation resistance and exceptional corrosion resistance make them attractive for high temperature applications [8,9]. However, the potential and advantage of secondary phase formation were shown in many HEAs in order to improve the mechanical properties [10–12]. For example, a combination of strength and ductility was achieved in well-known HEAs such as CoCrFeNiMn and $Al_{0.3}$CoCrFeNi due to formation of controlled amount of B2 phases in the FCC matrix or Laves phase formation in $CrFeNiNb_{0.158}$ HEA led to higher yield strength due to precipitation hardening mechanism [5] [11] [12]. Nevertheless, decomposition of HEAs in some temperature ranges leads to formation of undesirable precipitates such as formation of close-packed Frank–Kasper or topologically close- packed (TCP) phases which significantly deteriorate ductility (e.g., formation of sigma and Laves phases in HEAs). These topologically close pack (TCP) phases, also known as Frank-Kasper (FK) phases, formed complex crystallographic structures which are classified into low and high polyhedral groups based on their coordination numbers (CN) referring to the number of atom centering the polyhedron [13,14]. There are some reports on the effect of these hard brittle phases on improving the

strength, hardness, and wear resistance of HEAs at the expense of reducing ductility [10,15].

RHEAs inherently have a high potential to form TCP phases such as sigma (σ), mu (μ) , or Laves phases due to their constituent elements during solidification or after exposure to specific temperature range [16–18]. These phases have an important role on the physical and mechanical properties of RHEAs. Among TCP crystal structures, Laves phase with AB_2-type stoichiometry which crystallize with the hexagonal C14 ($MgZn_2$) structure, the cubic C15 ($MgCu_2$) structure, or the dihexagonal C36 ($MgNi_2$) structure are the most frequent intermetallic compounds in these alloys [19,20]. The coordination numbers (CN) of Frank–Kasper polyhedra in AB_2 Lave phase contain 16 for the larger A atoms and 12 for the smaller B atoms [19]. These Laves phase may deteriorate the mechanical properties due to their noticeable hardness and brittleness [19,21]. However, there are some reports denoting advantages of Laves phases on enhancement of the high- temperature strength and creep-strengthening of high-temperature alloys [19,22]. Furthermore, these phases proved to be beneficial in some applications, including being utilized as magneto- mechanical sensors, wear-and-corrosion-resistant coatings, superconducting materials and hydrogen storage material [19,23]. Formation of unwanted Laves phases in Superalloys as advanced material for high temperature applications like gas turbines, especially in Ni- and Co- based superalloys, have also been reported earlier which resulted in degradation of mechanical properties [24,25]. In contrast, a study on Inconel 718 showed a certain amount of small and granular Laves phase found to be beneficial for the room temperature tensile properties. It is worth noting that the influence of Laves phases in superalloys highly depends on sizes and morphologies of Laves phase precipitates [26]. It is well established that materials containing Laves phase have a potential for hydrogen storage material due to their appropriate tetrahedral interstitial sites and the possibility to form a Lave structure with elements having a

strong affinity for hydrogen (so- called A-type elements: Zr, Nb, V, etc.) [27]. In addition, Laves phases could significantly increase pathways for diffusion of hydrogen and lead to reversible hydrogenation, dehydrogenation and fast kinetics [28,29].

There are many factors that influence TCP phase formation in RHEAs including atomic size difference parameter (δ), mixing enthalpy (ΔH_{mix}) and Valence electron concentration (VEC) [30– 34]. The enthalpy of mixing and the difference in atomic size are decisive stable phase formation in HEA, however, VEC mainly affects the phase transition in HEA [34]. It is possible to encourage or suppress formation of TCP-Laves phase by controlling chemical composition according to the purpose of alloy design and intended application. Based on the above perspective on the importance of Laves phase formation on the behavior of RHEAs, the present investigation was conducted to address key parameters leading to TCP-Laves phase formation in RHEAs by considering thermodynamic calculations and empirical relations. Accordingly, two novel equiatomic RHEAs were designed, fabricated and studied to validate the related parameters on alloy design. It is a step forward to a fundamental understanding of RHEAs in order to apply microstructure and phase engineering to develop a high-performance material for different applications such as hydrogen storage and high temperature structural components.

2. Methodology

2.1. Empirical relations and thermodynamic aspects to predict Laves phase formation in RHEAs

Several thermodynamic parameters and critical values based on empirical relations have been proposed to predict the formation of different phases in HEAs, such as entropy of mixing (ΔS_{mix}), enthalpy of mixing (ΔH_{mix}), atomic radius difference (δ), and valence electron concentration (VEC) which are defined earlier [30–32,35–38]. It was well-established that a dual-phase HEA (solid solution together with an intermetallic compound) is expected to form

at $-20 \leq \Delta H_{mix} \leq -3$ kJ.mol^{-1} and $4 < \delta < 10$ [31,32]. The large δ leads to excess strain energy which leads to the instability of simple structures [5]. In addition, It have been reported that the BCC phases are stable in VEC⩽6.78, while the FCC solid-solution phases are stable at a VEC value larger than 8 [33]. It was expressed earlier that *d*-electron bonding is related to stability of TCP phases. The average value of the *d*-orbital energy level (M_d) is defined by following equation [39]:

$$\overline{M_d} = \sum_{i=1}^{n} c_i (M_d)_i, \quad (1)$$

where C_i is the atomic fraction of component *i* in the alloy, and $(M_d)_i$ is the d-orbital energy level of *i*th element [39,40]. These parameters were investigated to predict the formation of dual phase including BCC solid solution and intermetallic compounds in RHEAs considering the Ti, Zr, V, Cr, Fe and Co elements. Thermo-Calc 2019b software based on the CALculation of PHAse Diagrams (CALPHAD) method was used to predict the diagram phases as a function of temperature in quinary RHEAs.

2.2. Experimental methods

Transition elements of Ti, Zr, V, Cr, Fe and Co were utilized to make two equiatomic quinary alloys including TiVCrZrCo and TiVCrZrFe RHEAs. The alloys were fabricated by vacuum arc melting method. High-purity materials (>99.9%) were charged in a water-cooled copper crucible for alloy making with a total mass of ~30 g. The materials melted in the shape of a button, flipped and remelted several times to achieve acceptable homogeneity. Chemical composition of each alloy was examined using X-ray fluorescence (XRF) analysis under a vacuum atmosphere in Philips (PW2404) spectrometer. Phase constituents were determined using X-ray diffraction (XRD) employing Cu Kα radiation (wavelength λ = 0.154 nm) at 45 kV and a tube current of 200 mA. XRD measurements were performed over the 2θ range from 30°

to 80° using a Philips (X´pert MPD) diffractometer. Vickers microhardness measurements were taken under a load of 500 gf with a dwell time of 15 s. Each of the hardness values reported in this study represents the average of five individual measurements. Fracture toughness of the alloys was measured based on the Vickers microhardness measurements. The microstructural observations and chemical analyses of the alloys were carried out using a MIRA3 TESCAN field emission scanning electron microscopy (FE-SEM) equipped with Oxford Energy Dispersive X-Ray Spectrometer with a limit of detection over 5000 ppm. The samples were prepared for FE-SEM analysis by grinding up to 2500 grit SiC paper followed by polishing using a 300 nm alumina suspension to achieve a mirror-like surface finish.

3. Results

3.1. Alloy design and theoretical results

Figure 1 represents the atomic radius and the mixing enthalpy (ΔH_{mix}) of atom pairs between each constitutional element of Ti, Mo, Zr, Hf, V, Cr, W, Fe, Nb and Co [30,41]. It indicates that mixing enthalpy of Co with Nb, Hf, Ti and Zr elements and mixing enthalpy of Fe with Nb, Hf, and Zr elements shows very negative values (lower than -15 $kJ.mol^{-1}$) which promotes intermetallic compounds formation in alloys containing these elements [33]. An ideal radius ratio in the closest packing of Laves phase is $rA/rB < 1.225$ [42,43]. However, the actual size ratios of the atoms that form the binary Laves phase are between 1.05 and 1.70, for instance, the common $TiCr_2$, $ZrCo_2$ Lave phases have the atomic ratio of 1.13 and 1.28 respectively [44]. It is important to note that the δ parameter based on atomic radii is a key factor in Lave phase formation in multicomponent alloys. In addition, the atomic size factor is a key to realizing the site-substitution of elements in Laves phases, thus, higher atomic radii in Zr, Mo, Hf, Nb, W, and Ti refractory elements could places on A site, while lower atomic radii V, Co, Fe Cr

elements could substitute B site [26]. Basically, the addition of elements with high mixing enthalpies in HEA can lead to variations in phase stability and encourage formation of multiphase alloys [34]. For example, the mixing enthalpy atom pairs between Zr and Co refractory elements showed the most negative value with, -40.3.mol^{-1} which confirms the tendency of elements to form a compound. In addition, the higher atomic ratio facilitates the formation of TCP Laves phase, thereby, Zr and Hf elements with the highest atomic radii with 1.60 and 1.58 Å and Co, Cr and Fe with the lowest atomic radii with 1.25, 1.25, 1.24 Å have a higher probability to form intermetallic compounds. According to the above elements and noted parameters, two novel equiatomic TiVCrZrCo and TiVCrZrFe RHEAs were considered and fabricated as alloy models to validate the related parameters on alloy design and study the potential of TCP-phase formation.

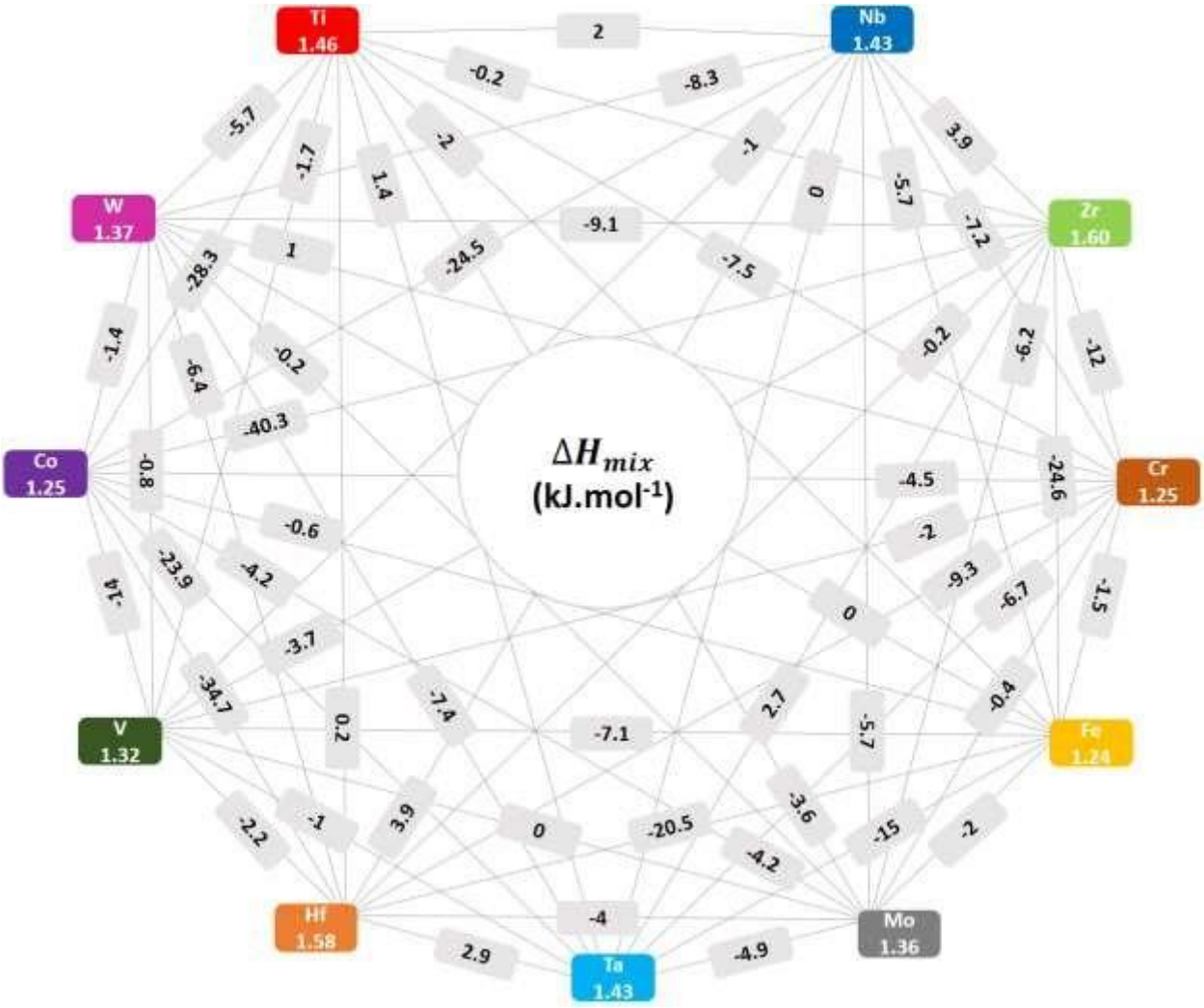

Fig. 1 The mixing enthalpy (ΔH_{mix}) in kJ.mol^{-1} of atom pairs between each constitutional element and atomic radii (Å) of each element.

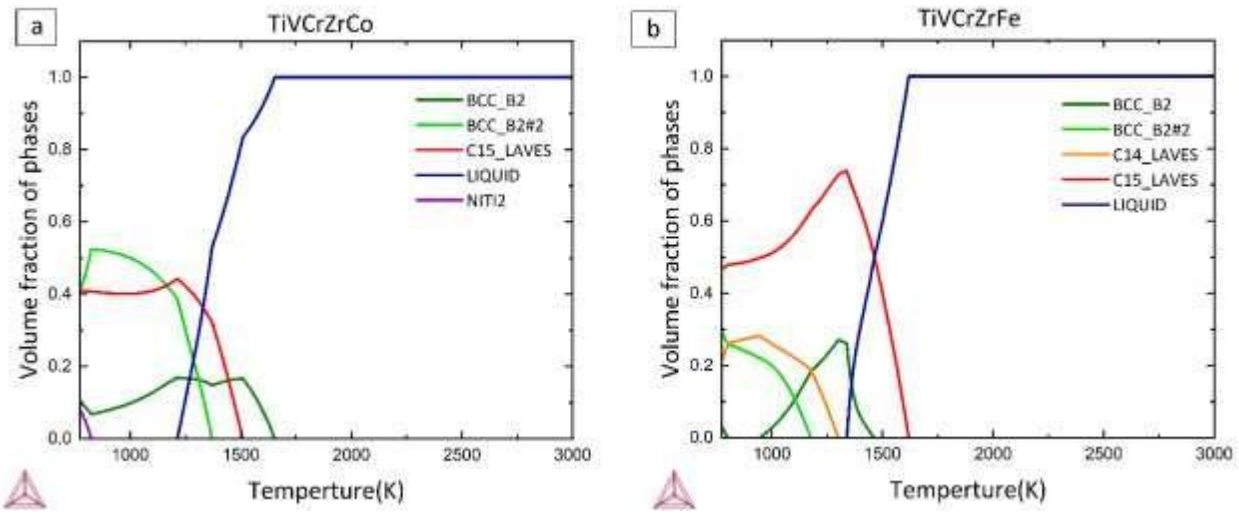

Fig. 2 Thermodynamic prediction diagrams of (a) TiVCrZrCo and (b) TiVCrZrFe RHEAs using Thermo-Calc software.

Figure 2 demonstrates the results of the Thermo-Calc predictions on phase formation and phase stability for TiVCrZrCo and TiVCrZrFe RHEAs at temperatures higher than 773 K. These predictions reveal multiple phases in a wide range of temperatures in both studied alloys. The results confirm the existence of the BCC phase together with TCP-Laves phases (C14 and C15) in both HEAs which the latter phases are stable up to the melting point. The C14 is hexagonal structure with space group *P*63/*mmc* and the C15 is face-centered cubic structure with space group *Fd3m*. The two types of Laves phase are related to each other due to different stackings of a basic unit [45]. Close inspection of results indicates formation of $NiTi_2$-type intermetallic compound which could be Ti_2Co in the Co-containing RHEA.

3.2. *Microstructure evaluation of fabricated RHEAs*

The chemical compositions of equiatomic TiVCrZrCo and TiVCrZrFe RHEAs were examined by XRF and EDS analyses and the results summarized in Table 1. The reported results clearly indicate that the chemical compositions of the fabricated RHEAs are very close to the nominal compositions. The XRD patterns of as-cast alloys represented in Fig. 3 confirm the

existence of the TCP-Laves phase together with BCC phase in the microstructures. In addition, two peaks corresponding to the Ti_2Co phase are visible in the XRD pattern of the TiVCrZrCo RHEAs which is in agreement with the thermodynamic predictions. Volume fraction and lattice parameter of detected phases were calculated and the results were summarized in Table 2. The volume fraction of phases were estimated from SEM micrograph using ImageJ software. As it is expected, the lattice parameter of intermetallic compounds including Laves phases are higher than BCC phase and the calculation confirms that volume fraction of BCC phase is higher than TCP Laves phases in both alloys.

Table 1 Chemical composition of RHEAs measured by XRF and EDS.

Nominal Composition (at%)		Chemical Composition(at%)					
		Ti	V	Cr	Zr	Fe	Co
$Ti_{20}Zr_{20}V_{20}Cr_{20}Fe_{20}$	XRF	20.9 ±0.3	17.6 ±1.0	21.4 ±0.9	21.1 ±0.4	19.0 ±0.8	_
	EDS	20.5 ±0.0	19.0 ±0.2	19.6 ±0.1	23.3 ±0.7	17.6 ±0.4	_
$Ti_{20}Zr_{20}V_{20}Cr_{20}Co_{20}$	XRF	23.7 ±0.5	16.9 ±1.0	17.4 ±0.3	20.7 ±0.0	_	21.4 ±1.2
	EDS	21.4 ±0.1	19.6 ±0.3	17.1 ±0.4	22.5 ±0.4	_	19.4 ±0.4

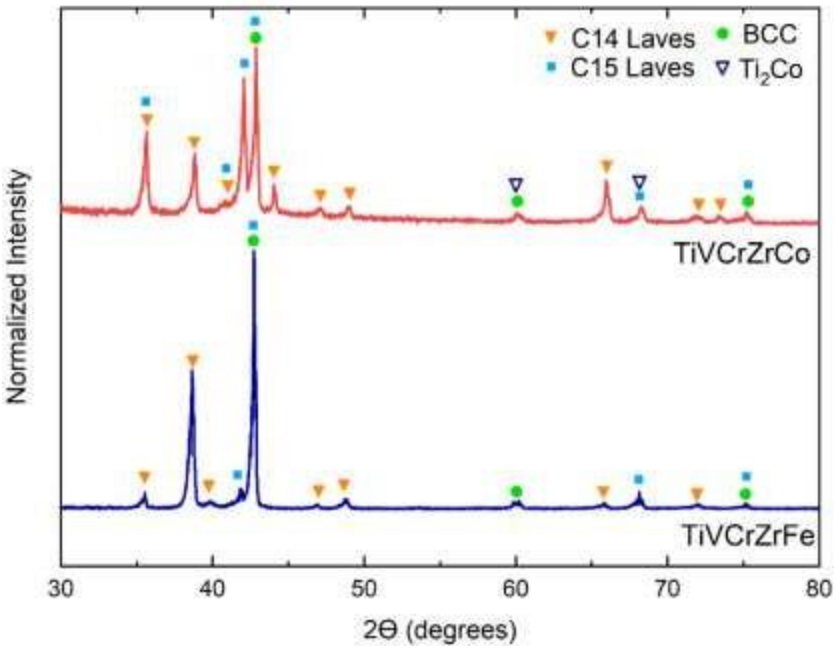

Fig. 3 X-ray diffraction patterns of designed alloys.

Table 2 Phase volume fraction and lattice parameters of detected phases in two RHEAs.

Alloy	Phase	Phase volume fraction (%)	Lattice parameter (Å)
TiVCrZrFe	BCC	57.82	2.991
	Laves phases	42.18	7.014*
TiVCrZrCo	BCC	60.80	3.035
	Laves phases	34.96	6.997*
	Ti_2Co	4.24	6.725

*Measured for C15 Laves phases

Figure 4 represents FE-SEM backscattered electron images of TiVCrZrCo and TiVCrZrFe RHEAs in the as-cast condition. These investigations show a cellular microstructure with two segregated phases at intercellular in both alloys. The higher magnification images together with EDS elemental maps are illustrated in Fig. 5. These elemental maps clearly reveal the partitioning of elements between cellular and intercellular regions with heavy elements Zr and Cr enriched at the cellular (bright phase) and lighter element Ti enriched at intercellular (dark

phase). However, homogenous distribution of V is visible in the microstructures of fabricated RHEAs. FE-SEM backscatter electron micrographs at higher magnification together with chemical analyses of the studied microstructures are illustrated in Fig. 6. The elemental concentrations for the different observed microstructures, as determined by EDX and given in at.%, are quoted in the figures for each region showed by arrows. These results show formation of two different Ti-rich phases including TCP-Laves phases and Ti_2Co phase in TiVCrZrCo at the intercellular region. The suggested stoichiometry of complex Lave phases are $(Zr,Ti)(Co,V,Cr,Ti)_2$ and $(Zr,Ti)(Fe,V,Cr,Ti)_2$ in TiVCrZrCo and TiVCrZrFe RHEAs, respectively. The present microstructural analyses show good agreement with XRD results and Thermo-Calc predictions.

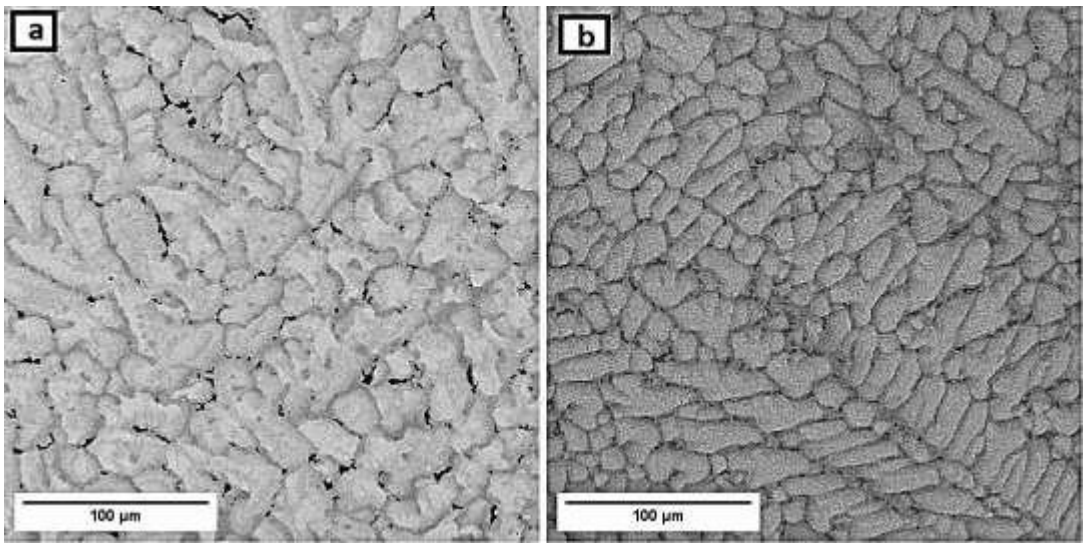

Fig. 4 FE-SEM backscatter electron images of (a) TiVCrZrFe and (b) TiVCrZrCo RHEAs.

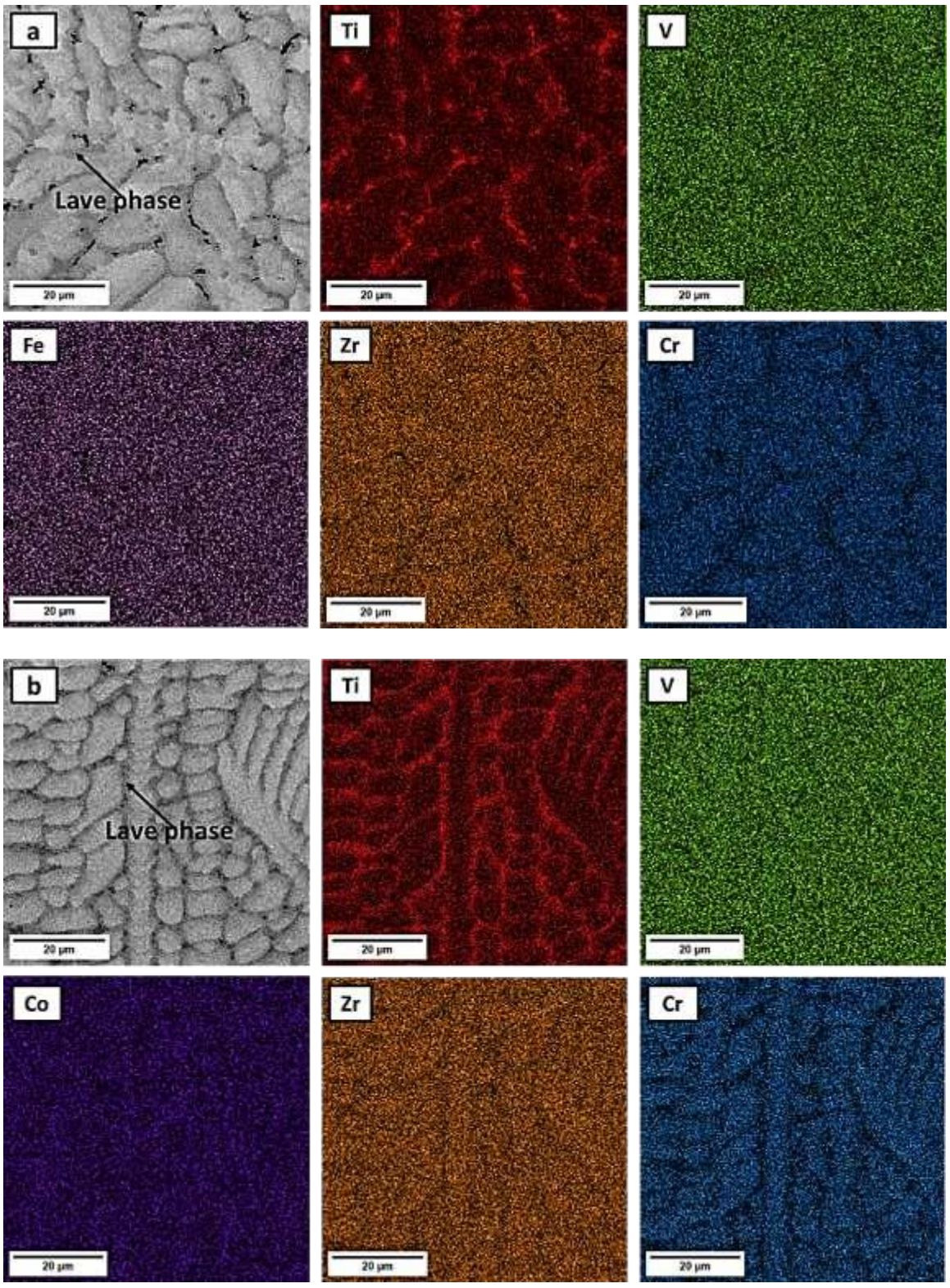

Fig. 5 SEM backscatter electron images together with corresponding EDS elemental maps of (a) TiVCrZrFe and (b) TiVCrZrCo RHEAs revealing distribution of elements in the microstructures.

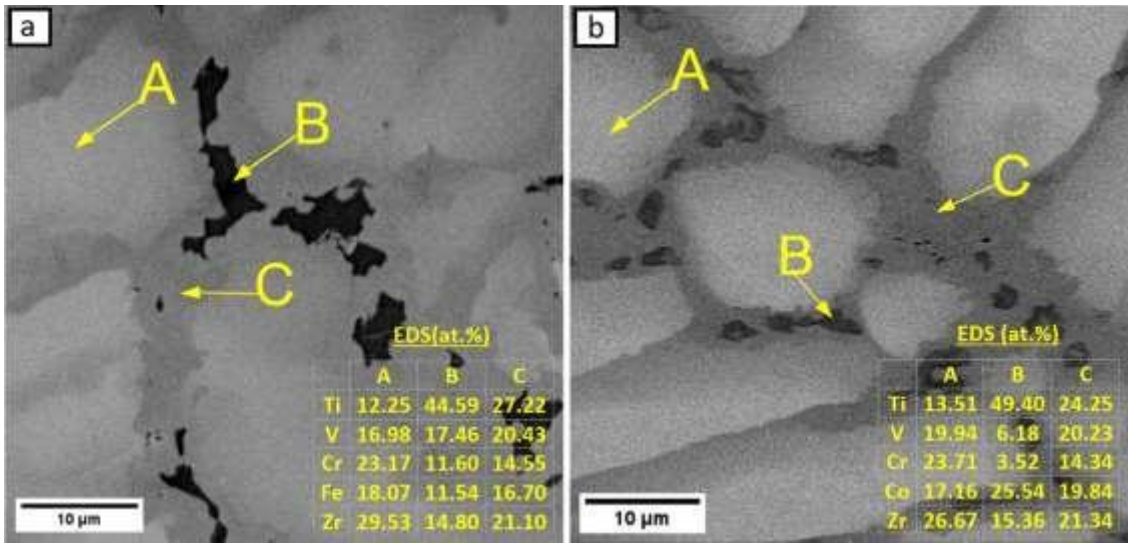

Fig. 6 Microstructure and chemical analyses of as-cast (a) TiVCrZrFe and (b) TiVCrZrCo RHEAs.

Microhardness measurements represent a high value of 748±17 and 692±24 Hv for TiVCrZrCo and TiVCrZrFe RHEAs, respectively. Complex microstructures including TCP phases are responsible to achieve such a high level of hardness in the investigated alloys. The fracture toughness values (*K*) for both RHEAs were calculated using the microhardness value from the following equation [46]:

$$K=0.016\left(\sqrt{E/H}\right) P/L^{3/2}$$

where *P* is the load, *H* the hardness value, *L* the average crack length and *E* the Young's modulus. It is important to note that the Young's modulus of each alloy was anticipated as 120 GPa using mixture rule [47–49]. The *L* value was taken from the average of four crack lengths at the corner of the five different indents from the optical micrograph (represented in Fig. 7). The formation of cracks during microhardness measurement confirms brittleness of two alloys due to the existence of a high volume fraction of TCP-Laves phase in the microstructures. The quadruple- phase TiVCrZrCo RHEA showed higher hardness and lower value of fracture toughness (1.18 $MPa.m^{0.5}$) compared with the triple-phase TiVCrZrFe RHEA (1.42 $MPa.m^{0.5}$).

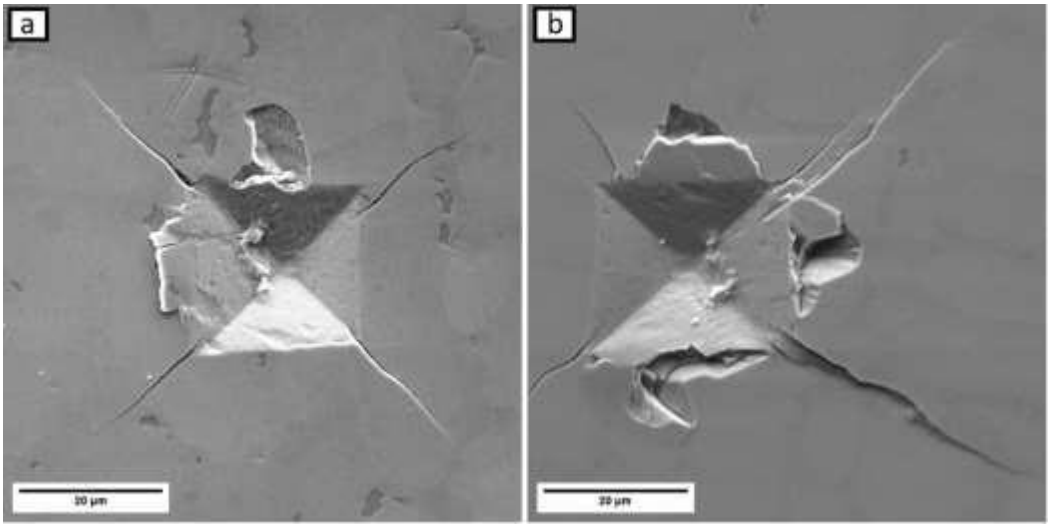

Fig. 7 Indentation deformation and cracks morphology in (a) TiVCrZrFe and (b) TiVCrZrCo.

4. Discussion

4.1. Correlation between microstructure and thermodynamic parameters

Prediction of phase formation in alloys such as TCP phases in RHEAs is the key factor in alloy designing based on requirements for the specific application. The thermodynamic parameters of entropy of mixing (ΔS_{mix}) and enthalpy of mixing (ΔH_{mix}), together with important elemental and physical functions of atomic δ, VEC, T_m (melting point) and ρ (density) were calculated for the designed and some other RHEAs and summarized in Table 3 in order to show the validation of the key parameters in prediction of phase formation in RHEAs [34,50]. It is important to note that melting point and density are two important parameters in RHEAs which fit them for high- temperature applications [51]. Studied RHEAs showed a wide range of densities from ~5.58 to 16.68 $g.cm^{-3}$, with most having a density of >8 $g.cm^{-3}$, which is almost higher than the density of conventional Ni-based superalloys alloys [52]. Accordingly, designing RHEAs with low densities, avoiding adding high density elements such as W, Ta and Mo is essential for making them ideal for potential applications of stationary structures or even

aerospace applications [53]. Close inspection of Table 3 reveals that the designed alloys in the present investigation show high melting points and relatively low densities. In addition, the presented results suggest that there is a good agreement between the melting points of alloys calculated by the rule of mixtures and Thermo-Calc predictions (Fig. 2). The calculated critical parameters including $-20 \leq \Delta H_{mix} \leq -3$ kJ.mol^{-1}, $4 < \delta < 10$ suggest formation of secondary phases in the designed RHEAs. According to the empirical value of δ, formation of multiphase microstructures containing TCP phases is expected in most of the alloys reported in Table 3. It is expected that the tendency of secondary phase formation increases by decreasing and increasing the ΔH_{mix} and δ values. The VEC value of RHEAs is less than 6.78 which indicates the formation of a BCC solid solution. It was reported earlier that a single-phase C14 Lave phase can form HEAs when the VEC value is 6 to 7 and C14 Lave phase coexists with the BCC phase is predictable when this value is lower than 6 [19,54– 59]. Close inspection Table 3 confirms this idea. However, it is reasonable to anticipate that the Laves-phase formation in HEAs is determined by difference between atomic sizes of the constitutive elements of the alloy [19,60]. In the case of the *d*-orbital energy level (M_d), it was reported that $M_d > 1.09$ leads to the formation of TCP phases in the microstructure [61]. The calculated M_d values for TiVCrZrCo and TiVCrZrFe RHEAs are 1.74 and 1.75 respectively, which suggest the formation of the TCP phase in both investigated alloys. The present investigation revealed that there is a good agreement between theoretical and empirical parameters in order to design RHEAs containing the TCP-Laves phase. The experiments and microstructural analyses together with Thermo-Calc predictions and physical functions shows formation of TCP Laves phase in the BCC solid-solution matrix in the two novel TiVCrZrCo and TiVCrZrFe RHEAs.

Table 3 Calculated parameters of ρ, T_m, ΔS_{mix}, ΔH_{mix}, VEC and δ for TiVCrZrCo and TiVCrZrFe and some RHEAs from previous studies [54-63].

Alloy	Phase	ρ ($g.cm^{-3}$)	T_m (K)	ΔS_{mix} ($J.k^{-1}.mol^{-1}$)	ΔH_{mix} ($KJ.mol^{-1}$)	VEC	δ	Refs.
TiVCrZrFe	BCC+C14+C15	6.44	2034	13.30	-12.34	5.4	10.02	This work
TiVCrZrCo	BCC+C14+C15+Ti_2Co	6.65	2036	13.30	-18.27	5.6	9.86	This work
AlCrNbTiV	BCC+C14	5.82	1982	13.30	-14.56	5.2	6.98	[62]
$Mo_{1.5}$NbTiVZr	BCC+C15	7.49	2426	13.23	-3.22	4.9	6.62	[63]
CrMoNbTiZr	BCC+C15	7.41	2366	13.30	-5.78	5	8.13	[64]
CrNbTiVZr	BCC+C15	6.58	2223	13.30	-4.70	5.4	9.73	[65]
CrHfNbTiZr	BCC+C15	8.02	2288	13.30	-4.22	4.6	8.63	[66]
$Cr_{0.3}Mo_{0.1}$NbTiZr	BCC+C15	7.10	2290	12.95	-6.69	5	8.89	[67]
$CrMo_{0.5}$NbTiV	BCC+C15	6.93	2295	13.18	-4.23	5.1	5.72	[68]
$Al_{0.5}CrNbTi_2V_{0.5}$	BCC+C14	5.85	2058	14.14	-11.04	4.6	5.88	[69]
TaNbHfZrTi	BCC	9.92	2515	13.30	13.79	4.4	6.96	[70]
VNbMoTaW	BCC	12.18	2959	13.30	-4.69	5.4	2.98	[71]

XRD results presented in Fig. 3 revealed two types of Laves phases including C14 and C15 in both RHEAs, however, Thermo-Calc predicted only C14 Laves phase in the TiVCrZrFe alloy. It was reported earlier that the hexagonal C14 has a higher flexibility to accommodate atoms of different sizes compared to the cubic C15 [19]. XRD results also showed two peaks of Ti_2Co intermetallic phase in TiVCrZrCo RHEAs which was predicted by Thermo-Calc results in Fig.2. The microstructural investigations of TiVCrZrCo and TiVCrZrFe RHEAs revealed cellular microstructures with TCP-Laves phase formed in the intercellular region. High solidification rates during the casting process may be important for the precipitation of these metastable AB_2 type Laves phase in the studied alloys.

4.2. Significance of topologically close-packed Laves phase

RHEAs have a potential to be considered as high-performance materials for different

applications such as high-temperature structural components or materials for hydrogen storage with fast kinetics and high cycling stability for reversible hydrogen storage [29,56]. However, this investigation reveals that there is a great tendency of TCP phase formation in these alloys which may affect the performance of them based on the application. Accordingly, the prediction of phase formation of different types of TCP-Laves phase is essential in RHEAs.

The formation of Laves phase occurs in AB_2 stoichiometry where *A* is a large atom (Ti, Zr, Hf, Nb, Ta) and *B* is a small atom (V, Mo, W, Fe, Cr, Co) [21,72,73]. Basically, very negative mixing enthalpy and the atomic size ratio in a range of 1.05-1.70 promotes Laves phase formation in binary systems [28,44]. These facts were reflected in Fig. 8 which clearly represents the tendency of Laves phase formation in RHEAs containing different constitutional elements. However, the chemical composition of Laves phases is more complicated due to availability of more elements in RHEAs. It was reported earlier in a ternary system that the Laves phase stoichiometry will be $(A_{1-x}C_x)(B_{1-y}C_y)_2$ when the possibility of *A* and *B* occupying the opposite sublattices will be neglected. For example, in $NbCr_2$ system, there is a preference for Ti for the *A* sites and Mo, W, V and Ti for the *B* sites [74]. Site preference of elements in Laves phases based on Nb-Cr-*C* systems indicates that Fe [75], Co [76] and Ni [77] substitute Cr on the *B* sites. In addition, the atoms with intermediate sizes like V, Mo and W [78] may occupy both *A* and *B* sites based on factors such as temperature or even on the presence of other elements [19]. Accordingly, complex compounds instead of binary intermetallic compounds are expected on TCP phases formed in RHEAs. For example, the Laves phase is not a fully binary $ZrCr_2$ in CrNbTiVZr RHEA and it contains other constitutional elements to form (Ti, Zr)(Cr, Nb, V)$_2$ indicating that part of the Cr has been replaced by V and Nb and part of the Zr has been substituted with Ti [79]. The complex Lave phase has been found in other RHEAs such as

$NbCrMo_{0.5}Ta_{0.5}TiZr$ [80] and TiZrNbFeNi [81] with (Zr, Ta)(Cr, Mo, Nb)$_2$ and (Zr, Ti)(Fe, Ni, Nb, Ti)$_2$ compositions, respectively. It is expected that Zr with a high atomic size of 1.60 Å occupies in *A* site and elements such as Co, Fe, V and Cr with lower atomic size (below 1.40 Å) occupy the B site. Apparently, Ti with intermediate atomic size of 1.43 Å occupies both *A* and *B* sites. According to the atomic size, represented in Fig. 1, it is expected that Laves phases of (Zr,Ti)(Co,V,Cr,Ti)$_2$ and (Zr,Ti)(Fe,V,Cr,Ti)$_2$ form in the designed TiVCrZrCo and TiVCrZrFe RHEAs, respectively, which are along with the experimental analyses.

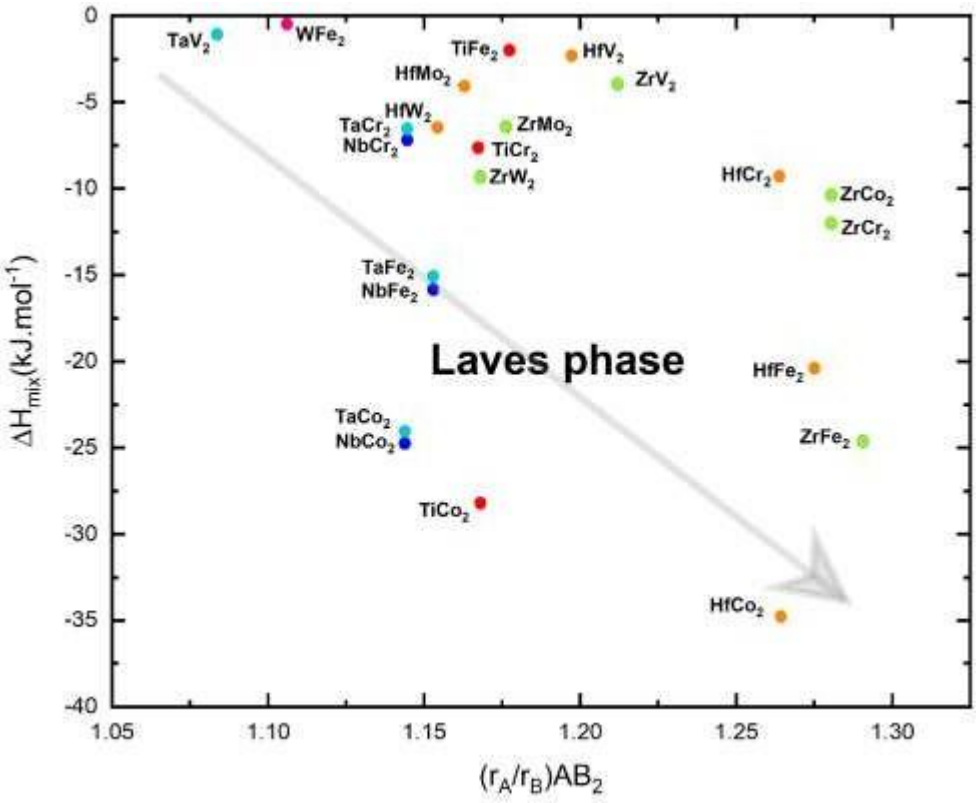

Fig. 8 Mixing Enthalpy (ΔH_{mix}) vs atomic size ratio (r_A/r_B) map for prediction of Laves phase formation in binary alloy system. Arrow shows tendency of the Laves phase formation.

The present results suggest that using refractory elements with big atomic radii such as Zr or Hf together with other elements with smaller atomic radii promotes formation of Laves phase in the RHEA (Fig. 8). Thereby, it is possible to manipulate the Laves phase type and its volume fraction in the microstructure by selecting appropriate type and atomic percentage of elements. Basically, controlling or in another word, engineering the volume fraction of the Lave phase is very effective on the mechanical and functional properties of RHEAs. Experimental data and thermodynamic simulations suggest that the volume fraction of Laves phase can be controlled either by adjusting the chemical composition of the alloy or by proper heat treatment [69,82][83,84]. RHEAs for hydrogen storage application such as TiZrNbFeNi and ZrTiVNiCrFe, usually contain major Laves phase (>80%), which results in lower hydride decomposition temperature and better reversibility with acceptance of storage capacity [81] [84] [85] [86]. In RHEAs in which the mechanical properties are the matter, it was reported the strength increases significantly by increasing the volume fraction of Laves phase, nevertheless, it deteriorates the ductility dramatically [87]. It was reported earlier that the strengthening ability of the AlCrNbTiZr RHEAs increases quickly when the volume fraction of Laves phases reaches to a critical value of ~30% [88]. Significant brittleness was reported earlier for single-Laves phase materials such as $ZrNbCr_2$ and $ZrHfCr_2$ with a fracture toughness of 1.01 and 1.05 $MPa.m^{0.5}$, respectively [89]. However, manipulating the chemical composition in order to form dual phase alloys containing BCC and Laves phase led to improved ductility and increased fracture toughness [90]. It is important to note that high hardness (>500 Hv) was reported for many multi-phase RHEAs such as $(TiVZrCr)_{90}W_{10}$ and $ZrNbTaCr_4Hf_{0.2}$ RHEAs contain more than 30% TCP phases [79,84]. Multi-phase TiVCrZrFe and TiVCrZrCo RHEAs show very high hardness (~690 and ~750 Hv, respectively) and low fracture toughness (1.42 and 1.18

$MPa.m^{0.5}$, respectively). Formation of Ti_2Co may be responsible for achieving higher hardness in the latter alloy. These RHEAs were designed based on the key factor in order to phase engineering and provide alloys with notable values of Laves phase (~40%) which can be interesting as hydrogen storage material or for applications in harsh operating environments exposed to high temperatures, irradiations, wear and erosion.

5. Summary and conclusions

1. The present study illustrated the role of key factors on designing RHEAs with or without TCP-Laves phases. Two novel TiVCrZrCo and TiVCrZrFe RHEAs were designed in order to apply phase engineering and provide alloys with notable values of Laves phase. The thermodynamic calculation using thermo-Cal and empirical calculations were conducted successfully to predict of Laves phase in TiVCrZrCo and TiVCrZrFe RHEAs and experimental investigations confirm the formation of ~40% TCP Laves phase in both RHEAs.

2. RHEAs inherently have a high potential to form TCP-Laves phase due to very negative values for mixing enthalpy of atom pairs and remarkable difference between atomic sizes of the constitutive elements of the alloy. Accordingly, existence of atoms such as V, Co, Cr and Fe together with Zr, Ti, Nb and Hf refractory elements promote TCP Laves phase formation. It is possible to manipulate the Laves phase type and its volume fraction or even suppress formation of these phases in the microstructure by selecting appropriate type and atomic percentage of elements.

3. Microstructural investigations showed BCC matrix together with C14 and C15 Laves phases for the TiVCrZrFe and quadruple-phase TiVCrZrCo alloy including BCC, C14, C15 and Ti_2Co phases. The stoichiometry of Laves phases are complex as $(Ti, Zr)(Co, V, Cr, Ti)_2$ and $(Ti, Zr)(Fe, V, Cr, Ti)_2$.

4. The designed RHEAs showed high melting point (>2000 K) and relatively low density (~6.5 $g.cm^{-3}$). High volume fraction of TCP-Laves phase in TiVCrZrFe and TiVCrZrCo RHEAs enhanced the strength significantly (hardness of ~700) at expense of decrease the ductility (low fracture toughness of <1.5 $MPa.m^{0.5}$). The understanding of key factors on RHEAs design leads to phase engineering and fabricated alloys with a desirable amount of TCP-Laves phase suited for hydrogen storage or high-temperature applications.

Acknowledgements

This work was supported by the Iran National Science Foundation (INSF) under Grant agreement no. 4006067.

References

[1] J. Chen, X. Zhou, W. Wang, B. Liu, Y. Lv, W. Yang, D. Xu, Y. Liu, A review on fundamental of high entropy alloys with promising high–temperature properties, J. Alloys Compd. 760 (2018) 15–30. https://doi.org/10.1016/j.jallcom.2018.05.067.

[2] S. Praveen, H.S. Kim, High-Entropy Alloys: Potential Candidates for High-Temperature Applications - An Overview, Adv. Eng. Mater. 20 (2018) 1700645. https://doi.org/10.1002/adem.201700645.

[3] J.-W. Yeh, S.-K. Chen, S.-J. Lin, J.-Y. Gan, T.-S. Chin, T.-T. Shun, C.-H. Tsau, S.-Y. Chang, Nanostructured High-Entropy Alloys with Multiple Principal Elements: Novel Alloy Design Concepts and Outcomes, Adv. Eng. Mater. 6 (2004) 299–303. https://doi.org/10.1002/adem.200300567.

[4] D.B. Miracle, O.N. Senkov, A critical review of high entropy alloys and related concepts, Acta Mater. 122 (2017) 448–511. https://doi.org/10.1016/j.actamat.2016.08.081.

[5] H. Shahmir, M.S. Mehranpour, S.A. Arsalan Shams, T.G. Langdon, Twenty years of the CoCrFeNiMn high-entropy alloy: achieving exceptional mechanical properties through microstructure engineering, J. Mater. Res. Technol. 23 (2023) 3362–3423. https://doi.org/10.1016/j.jmrt.2023.01.181.

[6] Y. Tong, L. Bai, X. Liang, M. Hua, J. Liu, Y. Li, J. Zhang, Y. Hu, Mechanical performance of (NbTaW)1−xMox (x = 0, 0.05, 0.15, 0.25) refractory high entropy alloys: Perspective from experiments and first principles calculations, J. Alloys Compd. 873 (2021) 159740. https://doi.org/10.1016/j.jallcom.2021.159740.

[7] Y. Lin, Y. Guo, Q. Dong, R. Huang, J. Tan, Effects of vanadium content on the high temperature oxidation behavior of NbTiZrAlV refractory complex concentrated alloys, J. Alloys Compd. 905 (2022) 164180. https://doi.org/10.1016/j.jallcom.2022.164180.

[8] B. Chen, L. Zhuo, Latest progress on refractory high entropy alloys: Composition, fabrication, post processing, performance, simulation and prospect, Int. J. Refract.

Met. Hard Mater. 110 (2023) 105993. https://doi.org/10.1016/j.ijrmhm.2022.105993.
[9] Z. Wang, S. Chen, S. Yang, Q. Luo, Y. Jin, W. Xie, L. Zhang, Q. Li, Light-weight refractory high-entropy alloys: A comprehensive review, J. Mater. Sci. Technol. 151 (2023) 41–65. https://doi.org/10.1016/j.jmst.2022.11.054.
[10] W.H. Liu, Z.P. Lu, J.Y. He, J.H. Luan, Z.J. Wang, B. Liu, Y. Liu, M.W. Chen, C.T. Liu, Ductile CoCrFeNiMox high entropy alloys strengthened by hard intermetallic phases, Acta Mater. 116 (2016) 332–342. https://doi.org/10.1016/j.actamat.2016.06.063.
[11] D. Choudhuri, B. Gwalani, S. Gorsse, M. Komarasamy, S.A. Mantri, S.G. Srinivasan, R.S. Mishra, R. Banerjee, Enhancing strength and strain hardenability via deformation twinning in fcc-based high entropy alloys reinforced with intermetallic compounds, Acta Mater. 165 (2019) 420–430. https://doi.org/10.1016/j.actamat.2018.12.010.
[12] D. Liang, C. Wei, F. Ren, Introducing Laves phase strengthening into an ultrafine-grained equiatomic CrFeNi alloy by niobium addition, Mater. Sci. Eng. A. 806 (2021) 140611. https://doi.org/10.1016/j.msea.2020.140611.
[13] F.C. Frank, J.S. Kasper, Complex alloy structures regarded as sphere packings. I. Definitions and basic principles, Acta Crystallogr. 11 (1958) 184–190. https://doi.org/10.1107/S0365110X58000487.
[14] C. Berne, M. Sluiter, A. Pasturel, Theoretical approach of phase selection in refractory metals and alloys, J. Alloys Compd. 334 (2002) 27–33. https://doi.org/10.1016/S0925- 8388(01)01773-X.
[15] M.-R. Chen, S.-J. Lin, J.-W. Yeh, M.-H. Chuang, S.-K. Chen, Y.-S. Huang, Effect of vanadium addition on the microstructure, hardness, and wear resistance of Al0.5CoCrCuFeNi high-entropy alloy, Metall. Mater. Trans. A. 37 (2006) 1363–1369. https://doi.org/10.1007/s11661-006-0081-3.
[16] A.N. Ladines, T. Hammerschmidt, R. Drautz, Structural stability of Fe-based topologically close-packed phases, Intermetallics. 59 (2015) 59–67. https://doi.org/10.1016/j.intermet.2014.12.009.
[17] K. Guruvidyathri, K.C. Hari Kumar, J.W. Yeh, B.S. Murty, Topologically Close-packed Phase Formation in High Entropy Alloys: A Review of Calphad and Experimental Results, JOM. 69 (2017) 2113–2124. https://doi.org/10.1007/s11837-017-2566-5.
[18] M. Ostrowska, G. Cacciamani, Thermodynamic modelling of the σ and μ phases in several ternary systems containing Co, Cr, Fe, Mo, Re and W, J. Alloys Compd. 845 (2020) 156122. https://doi.org/10.1016/j.jallcom.2020.156122.
[19] F. Stein, A. Leineweber, Laves phases: a review of their functional and structural applications and an improved fundamental understanding of stability and properties, J. Mater. Sci. 56 (2021) 5321–5427. https://doi.org/10.1007/s10853-020-05509-2.
[20] G. Sauthoff, Intermetallics, in: Ullmann's Encycl. Ind. Chem., Wiley-VCH Verlag GmbH & Co. KGaA, Weinheim, Germany, 2006. https://doi.org/10.1002/14356007.e14_e01.pub2.
[21] J. Nei, K. Young, S.O. Salley, K.Y.S. Ng, Determination of C14/C15 phase abundance in Laves phase alloys, Mater. Chem. Phys. 136 (2012) 520–527. https://doi.org/10.1016/j.matchemphys.2012.07.020.
[22] Y. Zhang, X. Chen, S. Jayalakshmi, R.A. Singh, V.B. Deev, E.S. Prusov, Factors determining solid solution phase formation and stability in CoCrFeNiX0.4 (X=Al, Nb, Ta) high entropy alloys fabricated by powder plasma arc additive manufacturing, J. Alloys Compd. 857 (2021) 157625. https://doi.org/10.1016/j.jallcom.2020.157625.
[23] J. Li, Y. Huang, X. Meng, Y. Xie, A Review on High Entropy Alloys Coatings: Fabrication Processes and Property Assessment, Adv. Eng. Mater. 21 (2019)

1900343. https://doi.org/10.1002/adem.201900343.
[24] A.S. Wilson, Formation and effect of topologically close-packed phases in nickel-base superalloys, Mater. Sci. Technol. 33 (2017) 1108–1118. https://doi.org/10.1080/02670836.2016.1187335.
[25] L. Wang, L. Song, A. Stark, Y. Liu, M. Oehring, U. Lorenz, F. Pyczak, Identification of Laves phases in a Zr or Hf containing γ-γ′ Co-base superalloy, J. Alloys Compd. 805 (2019) 880–886. https://doi.org/10.1016/j.jallcom.2019.07.121.
[26] S. Sui, H. Tan, J. Chen, C. Zhong, Z. Li, W. Fan, A. Gasser, W. Huang, The influence of Laves phases on the room temperature tensile properties of Inconel 718 fabricated by powder feeding laser additive manufacturing, Acta Mater. 164 (2019) 413–427. https://doi.org/10.1016/j.actamat.2018.10.032.
[27] J.-M. Joubert, C. Pommier, E. Leroy, A. Percheron-Guégan, Hydrogen absorption properties of topologically close-packed phases of the Nb–Ni–Al system, J. Alloys Compd. 356–357 (2003) 442–446. https://doi.org/10.1016/S0925-8388(02)01238-0.
[28] B. Cheng, Y. Li, X. Li, H. Ke, L. Wang, T. Cao, D. Wan, B. Wang, Y. Xue, Solid-State Hydrogen Storage Properties of Ti–V–Nb–Cr High-Entropy Alloys and the Associated Effects of Transitional Metals (M = Mn, Fe, Ni), Acta Metall. Sin. (English Lett. (2022). https://doi.org/10.1007/s40195-022-01403-9.
[29] A. Mohammadi, Y. Ikeda, P. Edalati, M. Mito, B. Grabowski, H.-W. Li, K. Edalati, High- entropy hydrides for fast and reversible hydrogen storage at room temperature: Binding- energy engineering via first-principles calculations and experiments, Acta Mater. 236 (2022) 118117. https://doi.org/10.1016/j.actamat.2022.118117.
[30] S. GUO, C.T. LIU, Phase stability in high entropy alloys: Formation of solid-solution phase or amorphous phase, Prog. Nat. Sci. Mater. Int. 21 (2011) 433–446. https://doi.org/10.1016/S1002-0071(12)60080-X.
[31] X. Yang, Y. Zhang, Prediction of high-entropy stabilized solid-solution in multi-component alloys, Mater. Chem. Phys. 132 (2012) 233–238. https://doi.org/10.1016/j.matchemphys.2011.11.021.
[32] Y.F. Ye, Q. Wang, J. Lu, C.T. Liu, Y. Yang, High-entropy alloy: challenges and prospects, Mater. Today. 19 (2016) 349–362. https://doi.org/10.1016/j.mattod.2015.11.026.
[33] B. Chanda, J. Das, An assessment on the stability of the eutectic phases in high entropy alloys, J. Alloys Compd. 798 (2019) 167–173. https://doi.org/10.1016/j.jallcom.2019.05.241.
[34] X. Chang, M. Zeng, K. Liu, L. Fu, Phase Engineering of High-Entropy Alloys, Adv. Mater. 32 (2020) 1–22. https://doi.org/10.1002/adma.201907226.
[35] L. Tan, K. Ali, P.S. Ghosh, A. Arya, Y. Zhou, R. Smith, P. Goddard, D. Patel, H. Shahmir, A. Gandy, Design principles of low-activation high entropy alloys, J. Alloys Compd. 907 (2022) 164526. https://doi.org/10.1016/j.jallcom.2022.164526.
[36] H.W. Yao, J.W. Qiao, J.A. Hawk, H.F. Zhou, M.W. Chen, M.C. Gao, Mechanical properties of refractory high-entropy alloys: Experiments and modeling, J. Alloys Compd. 696 (2017) 1139–1150. https://doi.org/10.1016/j.jallcom.2016.11.188.
[37] W. Huang, J. Hou, X. Wang, J. Qiao, Y. Wu, Excellent room-temperature tensile ductility in as-cast Ti37V15Nb22Hf23W3 refractory high entropy alloys, Intermetallics. 151 (2022) 107735. https://doi.org/10.1016/j.intermet.2022.107735.
[38] X.-W. Yang, X.-H. Shi, H.-J. Yang, J.-W. Qiao, P.K. Liaw, Y.-C. Wu, Entropy versus enthalpy in hexagonal-close-packed high-entropy alloys, Rare Met. 41 (2022) 2906–2920. https://doi.org/10.1007/s12598-022-02010-4.
[39] Y. Lu, Y. Dong, L. Jiang, T. Wang, T. Li, Y. Zhang, A Criterion for Topological Close- Packed Phase Formation in High Entropy Alloys, Entropy. 17 (2015) 2355–

2366. https://doi.org/10.3390/e17042355.
[40] M. Morinaga, N. Yukawa, H. Adachi, Alloying Effect on the Electronic Structure of Ni3Al (γ'), J. Phys. Soc. Japan. 53 (1984) 653–663. https://doi.org/10.1143/JPSJ.53.653.
[41] A. Takeuchi, A. Inoue, Mixing enthalpy of liquid phase calculated by miedema's scheme and approximated with sub-regular solution model for assessing forming ability of amorphous and glassy alloys, Intermetallics. 18 (2010) 1779–1789. https://doi.org/10.1016/j.intermet.2010.06.003.
[42] R. Nesper, A. Chemie, E.T. Hochschule, A covalent view of chemical bonding in Laves phases CaLixAl2 _ x, 197 (1993) 109–121.
[43] P. Formation, A Thermodynamic Interpretation of the Size-Ratio Limits for Laves Phase Formation, 30 (1999) 1–4.
[44] F. Stein, M. Palm, G. Sauthoff, Structure and stability of Laves phases . Part I . Critical assessment of factors controlling Laves phase stability, 12 (2004) 713–720. https://doi.org/10.1016/j.intermet.2004.02.010.
[45] X. Chen, W. Wolf, R. Podloucky, P. Rogl, Ab initio study of ground-state properties of the Laves phase compounds, (2005) 1–11. https://doi.org/10.1103/PhysRevB.71.174101.
[46] T. Ohta, Y. Kaneno, H. Inoue, S. Hanada, T. Takasugi, Phase Field and Room-Temperature Mechanical Properties of the C15 Laves Phase in the Zr-Ta-Cr Alloy System, 36 (2005).
[47] E. Fazakas, V. Zadorozhnyy, L.K. Varga, A. Inoue, D. V. Louzguine-Luzgin, F. Tian, L. Vitos, Experimental and theoretical study of Ti20Zr20Hf 20Nb20X20 (X = v or Cr) refractory high-entropy alloys, Int. J. Refract. Met. Hard Mater. 47 (2014) 131–138. https://doi.org/10.1016/j.ijrmhm.2014.07.009.
[48] O.N. Senkov, D.B. Miracle, K.J. Chaput, J.P. Couzinie, Development and exploration of refractory high entropy alloys - A review, J. Mater. Res. 33 (2018) 3092–3128. https://doi.org/10.1557/jmr.2018.153.
[49] H.W. Yao, J.W. Qiao, J.A. Hawk, H.F. Zhou, M.W. Chen, M.C. Gao, Mechanical properties of refractory high-entropy alloys: Experiments and modeling, J. Alloys Compd. 696 (2017) 1139–1150. https://doi.org/10.1016/j.jallcom.2016.11.188.
[50] Z.-S. Nong, J.-C. Zhu, Y. Cao, X.-W. Yang, Z.-H. Lai, Y. Liu, Stability and structure prediction of cubic phase in as cast high entropy alloys, Mater. Sci. Technol. 30 (2014) 363–369. https://doi.org/10.1179/1743284713Y.0000000368.
[51] J. Wadsworth, T.G. Nieh, J.J. Stephens, Recent advances in aerospace refractory metal alloys, 33 (1988).
[52] Z.Q. Xu, X.W. Cheng, M. Wang, Y.W. Chen, Y.D. Tan, X.W. Cheng, M. Wang, Y.W. Chen, Y.D. Tan, Design of novel low-density refractory high entropy alloys for high temperature applications, (2019). https://doi.org/10.1016/j.msea.2019.03.054.
[53] O.N. Senkov, S. V Senkova, C. Woodward, D.B. Miracle, Low-density , refractory multi- principal element alloys of the Cr – Nb – Ti – V – Zr system : Microstructure and phase analysis, ACTA Mater. (2012). https://doi.org/10.1016/j.actamat.2012.11.032.
[54] V.F. Gorban', N.A. Krapivka, S.A. Firstov, High-entropy alloys: Interrelations between electron concentration, phase composition, lattice parameter, and properties, Phys. Met. Metallogr. 118 (2017) 970–981. https://doi.org/10.1134/S0031918X17080051.
[55] Y.-F. Kao, S.-K. Chen, J.-H. Sheu, J.-T. Lin, W.-E. Lin, J.-W. Yeh, S.-J. Lin, T.-H. Liou, C.-W. Wang, Hydrogen storage properties of multi-principal-component CoFeMnTixVyZrz alloys, Int. J. Hydrogen Energy. 35 (2010) 9046–9059. https://doi.org/10.1016/j.ijhydene.2010.06.012.

[56] P. Edalati, R. Floriano, A. Mohammadi, Y. Li, G. Zepon, H.-W. Li, K. Edalati, Reversible room temperature hydrogen storage in high-entropy alloy TiZrCrMnFeNi, Scr. Mater. 178 (2020) 387–390. https://doi.org/10.1016/j.scriptamat.2019.12.009.
[57] T.P. Yadav, S. Mukhopadhyay, S.S. Mishra, N.K. Mukhopadhyay, O.N. Srivastava, Synthesis of a single phase of high-entropy Laves intermetallics in the Ti–Zr–V–Cr–Ni equiatomic alloy, Philos. Mag. Lett. 97 (2017) 494–503. https://doi.org/10.1080/09500839.2017.1418539.
[58] S. Guo, C. Ng, J. Lu, C.T. Liu, Effect of valence electron concentration on stability of fcc or bcc phase in high entropy alloys, J. Appl. Phys. 109 (2011) 103505. https://doi.org/10.1063/1.3587228.
[59] H.J. Park, Y.S. Na, S.H. Hong, J.T. Kim, Y.S. Kim, K.R. Lim, J.M. Park, K.B. Kim, Phase evolution, microstructure and mechanical properties of equi-atomic substituted TiZrHfNiCu and TiZrHfNiCuM (M = Co, Nb) high-entropy alloys, Met. Mater. Int. 22 (2016) 551–556. https://doi.org/10.1007/s12540-016-6034-5.
[60] H. Yao, D. Qiao, J. Miao, J. Wang, E. Guo, Criteria for laves-phase formation in refractory high-entropy alloys, 102 (2022) 161–177.
[61] M. Morinaga, N. Yukawa, H. Ezaki, H. Adachi, Solid solubilities in transition-metal-based f.c.c. alloys, Philos. Mag. A. 51 (1985) 223–246. https://doi.org/10.1080/01418610.1985.12069159.
[62] N.D. Stepanov, N.Y. Yurchenko, E.S. Panina, M.A. Tikhonovsky, S.V. Zherebtsov, Precipitation-strengthened refractory Al 0.5 CrNbTi 2 V 0.5 high entropy alloy, Mater. Lett. 188 (2017) 162–164. https://doi.org/10.1016/j.matlet.2016.11.030.
[63] Y.D. Wu, Y.H. Cai, X.H. Chen, T. Wang, J.J. Si, L. Wang, Y.D. Wang, X.D. Hui, Phase composition and solid solution strengthening effect in TiZrNbMoV high-entropy alloys, Mater. Des. 83 (2015) 651–660. https://doi.org/10.1016/j.matdes.2015.06.072.
[64] C. Xiang, E.-H. Han, Z.M. Zhang, H.M. Fu, J.Q. Wang, H.F. Zhang, G.D. Hu, Design of single-phase high-entropy alloys composed of low thermal neutron absorption cross-section elements for nuclear power plant application, Intermetallics. 104 (2019) 143–153. https://doi.org/10.1016/j.intermet.2018.11.001.
[65] O.N. Senkov, S.V. Senkova, D.B. Miracle, C. Woodward, Mechanical properties of low- density, refractory multi-principal element alloys of the Cr–Nb–Ti–V–Zr system, Mater. Sci. Eng. A. 565 (2013) 51–62. https://doi.org/10.1016/j.msea.2012.12.018.
[66] É. Fazakas, V. Zadorozhnyy, L.K. Varga, A. Inoue, D.V. Louzguine-Luzgin, F. Tian, L. Vitos, Experimental and theoretical study of Ti20Zr20Hf20Nb20X20 (X = V or Cr) refractory high-entropy alloys, Int. J. Refract. Met. Hard Mater. 47 (2014) 131–138. https://doi.org/10.1016/j.ijrmhm.2014.07.009.
[67] O.A. Waseem, U. Auyeskhan, H.M. Lee, H.J. Ryu, A combinatorial approach for the synthesis and analysis of Al x Cr y Mo z NbTiZr high-entropy alloys: Oxidation behavior, J. Mater. Res. 33 (2018) 3226–3234. https://doi.org/10.1557/jmr.2018.241.
[68] C. Xiang, H.M. Fu, Z.M. Zhang, E. Han, H.F. Zhang, J.Q. Wang, G.D. Hu, Effect of Cr content on microstructure and properties of Mo 0.5 VNbTiCr x high-entropy alloys, 818 (2020). https://doi.org/10.1016/j.jallcom.2019.153352.
[69] N.D. Stepanov, N.Y. Yurchenko, D.V. Skibin, M.A. Tikhonovsky, G.A. Salishchev, Structure and mechanical properties of the AlCrxNbTiV (x = 0, 0.5, 1, 1.5) high entropy alloys, J. Alloys Compd. 652 (2015) 266–280. https://doi.org/10.1016/j.jallcom.2015.08.224.
[70] O.N. Senkov, J.M. Scott, S. V. Senkova, F. Meisenkothen, D.B. Miracle, C.F. Woodward, Microstructure and elevated temperature properties of a refractory

TaNbHfZrTi alloy, J. Mater. Sci. 47 (2012) 4062–4074. https://doi.org/10.1007/s10853-012-6260-2.
[71] O.N. Senkov, G.B. Wilks, J.M. Scott, D.B. Miracle, Mechanical properties of Nb25Mo25Ta 25W25 and V20Nb20Mo 20Ta20W20 refractory high entropy alloys, Intermetallics. 19 (2011) 698–706. https://doi.org/10.1016/j.intermet.2011.01.004.
[72] C.D. Rabadia, Y.J. Liu, L. Wang, H. Sun, L.C. Zhang, Laves phase precipitation in Ti-Zr- Fe-Cr alloys with high strength and large plasticity, Mater. Des. 154 (2018) 228–238. https://doi.org/10.1016/j.matdes.2018.05.035.
[73] D.J. Thoma, J.H. Perepezko, A geometric analysis of solubility ranges in Laves phases, J. Alloys Compd. 224 (1995) 330–341. https://doi.org/10.1016/0925-8388(95)01557-4.
[74] H. Okaniwa, D. Shindo, M. Yoshida, T. Takasugi, Determination of site occupancy of additives X (X=V, Mo, W and Ti) in the Nb–Cr–X Laves phase by ALCHEMI, Acta Mater. 47 (1999) 1987–1992. https://doi.org/10.1016/S1359-6454(99)00065-8.
[75] A. Jacob, C. Schmetterer, D. Grüner, E. Wessel, B. Hallstedt, L. Singheiser, The Cr–Fe–Nb ternary system: Experimental isothermal sections at 700 °C, 1050 °C and 1350 °C, J. Alloys Compd. 648 (2015) 168–177. https://doi.org/10.1016/j.jallcom.2015.06.137.
[76] X. Zhang, S. Yang, C. Zhao, Y. Lu, X. Liu, C. Wang, Experimental Investigation of Phase Equilibria in the Co-Cr-Nb System at 1000, 1100, and 1200 °C, J. Phase Equilibria Diffus. 34 (2013) 313–321. https://doi.org/10.1007/s11669-013-0237-y.
[77] X. Nie, S. Lu, K.-L. Wang, T. Chen, C. Niu, Fabrication and toughening of NbCr2 matrix composites alloyed with Ni obtained by powder metallurgy, Mater. Sci. Eng. A. 502 (2009) 85–90. https://doi.org/10.1016/j.msea.2008.10.004.
[78] Z. Wei, Y. Yang, J. Huang, B. Wu, B. Sa, Y. Huang, S. Wang, M. Lin, C.-T. Tsai, K. Bai, Prediction of site occupancy of C15 Laves phase at finite temperature based on quasi- harmonic approximation model, Intermetallics. 96 (2018) 33–40. https://doi.org/10.1016/j.intermet.2018.02.007.
[79] H. Wang, K. Xu, J. Zhang, J. Zhang, Microstructure and Mechanical Properties of High- Specific-Strength (TiVCrZr)100−xWx (x = 5, 10, 15 and 20) Refractory High-Entropy Alloys, Entropy. 25 (2023) 100. https://doi.org/10.3390/e25010100.
[80] O.N. Senkov, C.F. Woodward, Microstructure and properties of a refractory NbCrMo0.5Ta0.5TiZr alloy, Mater. Sci. Eng. A. 529 (2011) 311–320. https://doi.org/10.1016/j.msea.2011.09.033.
[81] R. Floriano, G. Zepon, K. Edalati, G.L.B.G. Fontana, A. Mohammadi, Z. Ma, H.-W. Li, R.J. Contieri, Hydrogen storage in TiZrNbFeNi high entropy alloys, designed by thermodynamic calculations, Int. J. Hydrogen Energy. 45 (2020) 33759–33770. https://doi.org/10.1016/j.ijhydene.2020.09.047.
[82] X. Yang, S.Y. Chen, J.D. Cotton, Y. Zhang, Phase Stability of Low-Density, Multiprincipal Component Alloys Containing Aluminum, Magnesium, and Lithium, JOM. 66 (2014) 2009–2020. https://doi.org/10.1007/s11837-014-1059-z.
[83] N.Y. Yurchenko, N.D. Stepanov, D.G. Shaysultanov, M.A. Tikhonovsky, G.A. Salishchev, Effect of Al content on structure and mechanical properties of the AlxCrNbTiVZr (x = 0; 0.25; 0.5; 1) high-entropy alloys, Mater. Charact. 121 (2016) 125–134. https://doi.org/10.1016/j.matchar.2016.09.039.
[84] L. Fang, J. Wang, X. Li, X. Tao, Y. Ouyang, Y. Du, Effect of Cr content on microstructure characteristics and mechanical properties of ZrNbTaHf0.2Crx refractory high entropy alloy, J. Alloys Compd. 924 (2022) 166593. https://doi.org/10.1016/j.jallcom.2022.166593.

[85] V. Zadorozhnyy, B. Sarac, E. Berdonosova, T. Karazehir, A. Lassnig, C. Gammer, M. Zadorozhnyy, S. Ketov, S. Klyamkin, J. Eckert, Evaluation of hydrogen storage performance of ZrTiVNiCrFe in electrochemical and gas-solid reactions, Int. J. Hydrogen Energy. 45 (2020) 5347–5355. https://doi.org/10.1016/j.ijhydene.2019.06.157.
[86] L. Huang, M. Long, W. Liu, S. Li, Effects of Cr on microstructure, mechanical properties and hydrogen desorption behaviors of ZrTiNbMoCr high entropy alloys, Mater. Lett. 293 (2021) 129718. https://doi.org/10.1016/j.matlet.2021.129718.
[87] S.G. Ma, Y. Zhang, Effect of Nb addition on the microstructure and properties of AlCoCrFeNi high-entropy alloy, Mater. Sci. Eng. A. 532 (2012) 480–486. https://doi.org/10.1016/j.msea.2011.10.110.
[88] N. Yurchenko, E. Panina, S. Zherebtsov, N. Stepanov, Design and characterization of eutectic refractory high entropy alloys, Materialia. 16 (2021) 101057. https://doi.org/10.1016/j.mtla.2021.101057.
[89] Y. Nakagawa, T. Ohta, Y. Kaneno, H. Inoue, T. Takasugi, Defect structures and room- temperature mechanical properties of C15 Laves phases in Zr-Nb-Cr and Zr-Hf-Cr alloy systems, Metall. Mater. Trans. A Phys. Metall. Mater. Sci. 35 A (2004) 3469–3476. https://doi.org/10.1007/s11661-004-0184-7.
[90] M. Fujita, Y. Kaneno, T. Takasugi, Phase field and room-temperature mechanical properties of C15 Laves phase in Nb-Hf-Cr and Nb-Ta-Cr alloy systems, J. Alloys Compd. 424 (2006) 283–288. https://doi.org/10.1016/j.jallcom.2005.11.087.